Volume 1
Number 5
November 2024
Pages 425–554

RSC Mechanochemistry

rsc.li/RSCMechanochem

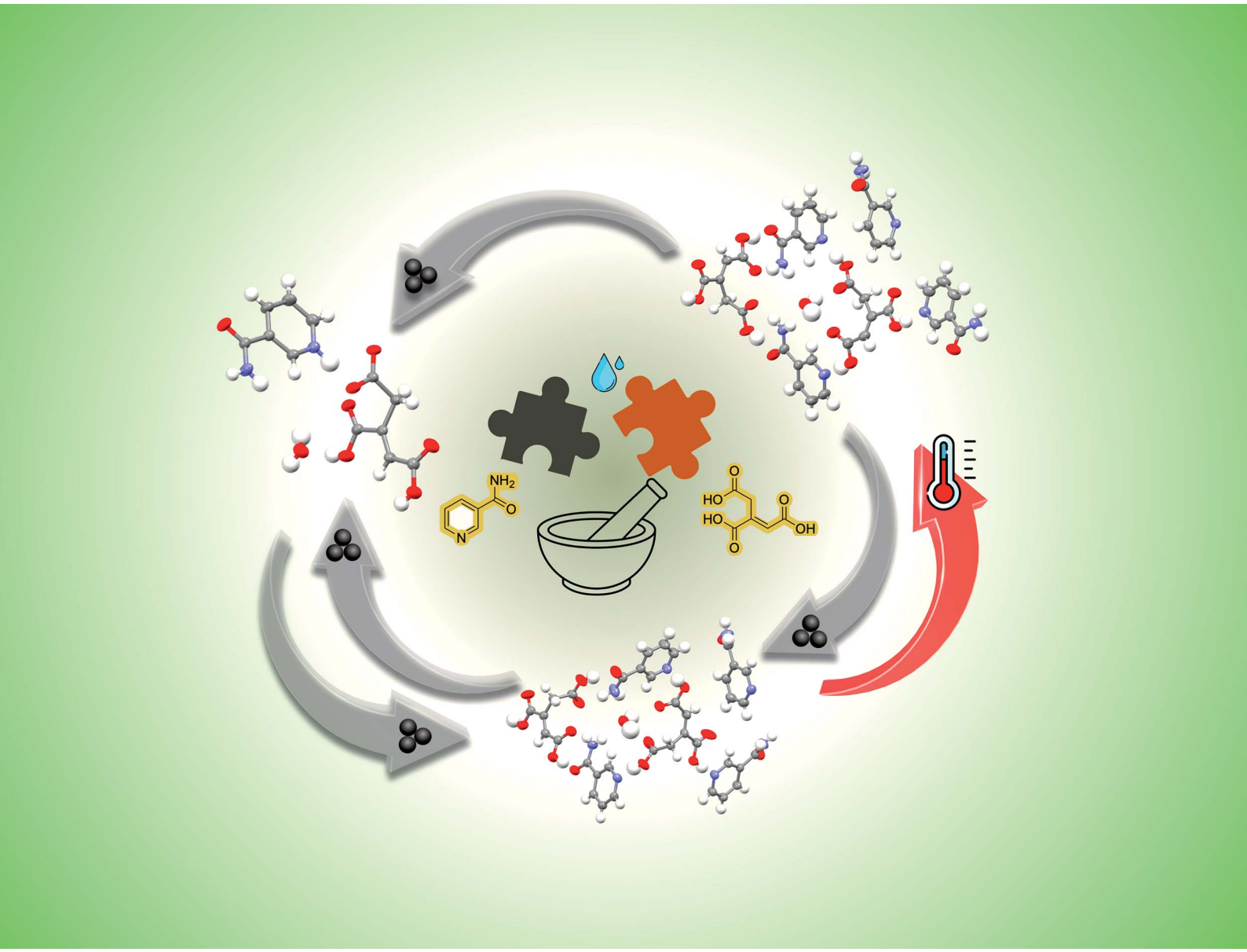

ISSN 2976-8683

ROYAL SOCIETY OF CHEMISTRY

PAPER

Ramesh Ch Deka, Ranjit Thakuria *et al.*
Exploring polymorphism, stoichiometric diversity and simultaneous existence of salt and cocrystal during cocrystallization using mechanochemistry

RSC Mechanochemistry

ROYAL SOCIETY OF CHEMISTRY

PAPER

View Article Online
View Journal | View Issue

Cite this: *RSC Mechanochem.*, 2024, **1**, 452

Exploring polymorphism, stoichiometric diversity and simultaneous existence of salt and cocrystal during cocrystallization using mechanochemistry†

Diptajyoti Gogoi,[a] Kalyan J. Kalita,[b] Nishant Biswakarma,[c] Mihails Arhangelskis,[d] Ramesh Ch Deka *[c] and Ranjit Thakuria *[a]

Received 22nd November 2023
Accepted 5th July 2024

DOI: 10.1039/d3mr00022b

rsc.li/RSCMechanochem

We demonstrate here the mechanochemical cocrystallization of *trans*-aconitic acid (TACA) with nicotinamide (NA) that leads to the formation of multi-component crystal forms with stoichiometric diversity, polymorphism with high Z'' and the simultaneous existence of salt and cocrystal. During cocrystallization, we obtained a 1 : 1 molecular salt hydrate of TACA with NA and two polymorphic cocrystal hydrates of the same in 1 : 2 ratios, with a Z'' value of seven, respectively. Manual grinding shows that 1 : 1 molecular salt and 1 : 2 cocrystal polymorphs are interconvertible under appropriate conditions. Moreover, cocrystal dissociation was observed upon heating the 1 : 2 cocrystal and in the presence of excess TACA during the preparation of the form I cocrystal using LAG. Thermal analysis, powder XRD, and DFT calculations establish the relative stability of the multi-component solids. Three-component polymorphic systems with high Z'' are quite unusual; however, based on mechanochemistry, we have successfully synthesized and characterized them.

Introduction

In the recent past, mechanochemistry, *i.e.*, chemical reactions induced by mechanical agitation such as grinding, milling, crushing, and shearing, has gained tremendous attention due to its clean and green method of preparation. This is the reason why IUPAC in 2019 acknowledged mechanochemistry as one of the top 10 emerging technologies in chemistry, which will contribute to the well-being of society and to a sustainable planet Earth.[1] As mechanochemical reactions take place under non-equilibrium conditions, there is always a possibility for the formation of kinetically "trapped" metastable polymorphic phases.[2,3] Moreover, there are several factors that can influence the outcome of a mechanochemical transformation compared to solution-phase crystallization.[2,4] Some of the factors discussed in the literature include the material of the milling jar,[5–7] the frequency of vibration,[8–10] the presence/nature of additives (liquid or solid),[3,11–15] the amount of liquid additives (η) used during grinding (liquid assisted grinding, LAG),[16] the number of balls used during milling,[17,18] ball size or ball mass,[19] milling temperature,[20] *etc.* During the last few decades, new mechanochemical techniques have also been developed like resonance acoustic mixing (RAM),[21] speed mixing,[22] *etc.* In addition to organic synthesis[23–25] and the preparation of metal–organic frameworks (MOFs)[26–28] or covalent organic frameworks (COFs),[29–31] mechanochemistry has widely been used to prepare multi-component molecular solids,[32,33] such as cocrystals, salts, solvates and/or hydrates. The classification of cocrystals as a new type of crystal form by the Food and Drug Administration (FDA) resulted in pharmaceutical cocrystals gaining tremendous attention. Although cocrystallization might be a possible solution to achieving a specific physicochemical property, it increases the possibility of finding novel multi-component solid forms such as cocrystal solvates, cocrystal hydrates, ionic cocrystals, molecular solid-solutions, eutectics, polymorphs in multi-component solids, stoichiometric variations and so on.[34] Therefore, during the preparation of pharmaceutical cocrystals and salts, it is always recommended to explore all these possibilities in order to avoid the appearance of unwanted thermodynamic phases.[35,36] With respect to that, mechanochemistry is a very useful tool to investigate the possible solid-state landscape of single component as well as multi-component pharmaceutical solids.

Here in this manuscript, we have chosen a novel system consisting of *trans*-aconitic acid (TACA), a fundamental

[a]*Department of Chemistry, Gauhati University, Guwahati 781014, India. E-mail: ranjit.thakuria@gauhati.ac.in; ranjit.thakuria@gmail.com*

[b]*Department of Chemical Sciences, Indian Institute of Science Education and Research Kolkata, 741246, West Bengal, India*

[c]*Department of Chemical Sciences, Tezpur University, Tezpur, Assam, India. E-mail: ramesh@tezu.ernet.in*

[d]*Faculty of Chemistry, University of Warsaw, 1 Pasteura Street, 02-093 Warsaw, Poland*

† Electronic supplementary information (ESI) available: Extensive experimental section as well as PXRD patterns, crystallographic data table and optimized coordinates of individual conformers. CCDC 2291739–2291741 and 2355242. For ESI and crystallographic data in CIF or other electronic format see DOI: https://doi.org/10.1039/d3mr00022b

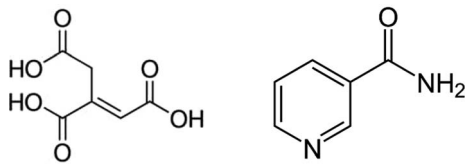

Scheme 1 Molecular structures of the two compounds: (a) *trans*-aconitic acid (TACA) and (b) nicotinamide (NA) used for co-crystallization.

metabolite, and nicotinamide (NA), also known as vitamin B3, which resulted in the formation of multi-component solids (salt as well as cocrystal) with stoichiometric diversity along with a pair of polymorphic cocrystal hydrates during mechanochemical synthesis (Scheme 1). In the literature, only one cocrystal of TACA with pyrazinamide is reported[37] along with the crystal structure of polymorphic anhydrous *cis*-aconitic acid[38,39] and its cocrystal with carbamazepine.[40] We used manual grinding in order to prepare all possible multi-component solids and to study their interconversion *via* a "one pot polymorph and variable stoichiometry turnover experiment". Moreover, we have investigated salt and cocrystal formation during variable stoichiometry co-crystallization experiments and compared the relative energies of the molecular salt hydrate and polymorphic cocrystal hydrate, based on density-functional theory (DFT) calculations.

Experimental

A description of some of the experimental procedures is given here; the ESI† provides experimental details on structure determination and DFT calculations.

Materials

All compounds used in this work were purchased from commercial sources and used without further purification.

Laboratory liquid-assisted grinding

Trans-aconitic acid (TACA) (MW 174.108 g mol^{-1}) and nicotinamide (NA) (MW 122.127 g mol^{-1}) were taken in 1 : 1 and 1 : 2 stoichiometric ratios and ground using a mortar and pestle in the presence of various added liquids for about 30 min, resulting in the formation of the respective salt and cocrystal. The resultant powder materials were examined using powder X-ray diffraction (PXRD).

Solution crystallization

The solution crystallization of all the salt and cocrystal of TACA and NA was carried out using powdered samples obtained from LAG with various laboratory solvents (acetonitrile, dioxane, ethanol, methanol, nitromethane, tetrahydrofuran, *etc.*) by placing around 30–40 mg of the powdered material in ~2–3 mL of the respective solvents and stirring until the solids disappeared. The clear solution (filtrate) was kept at room temperature for crystallization.

Powder X-ray diffraction (PXRD)

PXRD measurements were performed at room temperature on a Rigaku Ultima IV X-ray powder diffractometer operating with a Cu Kα X-ray source, equipped with a Ni filter to suppress Kβ emission and a D/teX Ultra-high-speed position sensitive detector, with a scan range $2\theta = 5$–50°, a step size of 0.02° and a scan rate of 10° min^{-1}.

Single crystal X-ray diffraction

The single crystal X-ray diffraction (SCXRD) data of all the salt and cocrystal were collected on a Bruker SMART APEX II CCD diffractometer equipped with a graphite monochromator and a Mo Kα fine-focus sealed tube ($\lambda = 0.71073$ Å). Data integration was done using SAINT. Intensities for absorption were corrected using SADABS.[41] Structure solution and refinement were carried out using Bruker SHELXL.[42] The hydrogen atoms were refined isotropically, and all the other atoms were refined anisotropically. C–H hydrogens were fixed using the HFIX command in SHELXL. Molecular graphics were prepared using X-SEED[43] and Mercury[44] licensed version 4.2.

Thermal analysis

Thermogravimetric analysis (TGA) measurements were performed on a Mettler Toledo instrument with a temperature range of 25–450 °C and a heating rate of 10 °C min^{-1}. Samples were placed in silica crucibles and purged with a stream of nitrogen flowing at 20 mL min^{-1}. DSC measurements were performed on a Mettler Toledo DSC instrument with a temperature range of 25–400 °C and heating rate of 10 °C min^{-1} on samples placed on a 40 μL aluminium pan with a pin-hole lid under an ultra-high pure nitrogen environment purged at 40 mL min^{-1}.

FESEM analysis

The morphology of TACA–NA–H_2O salt and cocrystal powder materials prepared using LAG was analyzed using a FESEM, Sigma-300, ZEISS.

Results and discussion

The reasons for the selection of the two compounds, namely *trans*-aconitic acid (TACA) and nicotinamide (NA), for this study are twofold: (1) due to the high propensity of acid–amide and acid–pyridine supramolecular synthons to form cocrystals[45,46] and (2) the number of available functional groups present in the two molecules, which might result in stoichiometric variation, the occurrence of high Z'' and/or the formation of polymorphic forms during grinding as well as solution crystallization.[47–52] Initially, TACA (87 mg, 0.5 mmol) and NA (61 mg, 0.5 mmol; 122.13 mg, 1 mmol) in 1 : 1 and 1 : 2 stoichiometric ratios were placed in a mortar and ground in the presence of 100 μL acetonitrile (ACN) as added liquid. PXRD of the resultant

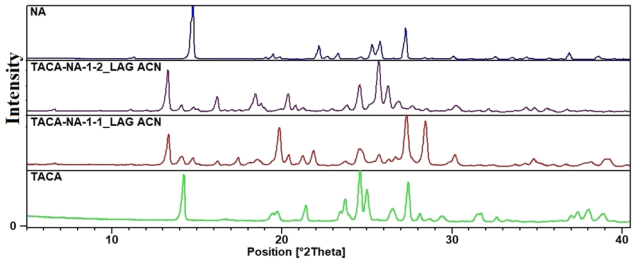

Fig. 1 Comparison of the powder patterns of 1 : 1 and 1 : 2 TACA–NA LAG samples showing well distinct powder patterns different from those of their respective starting materials.

powders shows well distinct powder patterns different from those of their respective starting materials, *viz.*, TACA and NA (Fig. 1). In order to characterize the materials, LAG samples were dissolved in 1 : 1 mixture solvent of THF and methanol, and allowed to evaporate slowly. After a period of one week, nice block shaped single crystals were obtained and used for single crystal X-ray diffraction analysis.

Crystal structure analysis showed that the 1 : 1 mixture of TACA–NA results in a $(TACA)^{-}\cdot(NA)^{+}\cdot(H_2O)$ 1 : 1 molecular salt of TACA and NA along with a water molecule in the asymmetric unit (Fig. 2a). Due to the formation of the molecular salt, SCXRD data were collected even at 100 K along with room temperature (298 K) in order to confirm the proton transfer from TACA to NA and the formation of the molecular salt. Also, the structural description is based on 100 K data in order to minimize the thermal vibration of atoms present in the salt structure. The crystal structure was solved in the monoclinic non-centrosymmetric *Cc* space group. One of the carboxylic acid protons of TACA was transferred to the N atom of the neighboring NA ring, resulting in the formation of a molecular salt. The relatively shorter C12–O6 bond (1.2893(1) Å) compared to C7–O2 (1.3295(1) Å) and C10–O4 (1.3149(1) Å) bonds of the other two carboxylic acid groups confirms the resonance stabilization of the carboxylate group and possible proton transfer from the TACA unit to the neighboring NA molecule. Moreover, the N2–H2B distance is 1.08(3) Å and the H2B···O6 distance is 1.47(4) Å (unnormalized distance), clearly depicting the transfer of the carboxylic acid proton from TACA to the NA molecule, resulting in the formation of a molecular salt. Looking into the CSD with an acid–pyridine hydrogen bond synthon, molecular salts with CSD ref code. MOVTEX (D = 2.533 Å), MOYSEZ (D = 2.57 Å), MUSQAV (D = 2.56 Å), OFESIB (D = 2.544), *etc.*, having a donor–acceptor distance (D) close to the TACA–NA 1 : 1 crystal structure having a D value of 2.551 Å (O6–N2) suggests possible proton transfer. Surprisingly, the resultant molecular salt does not contain the most abundant acid–amide ring synthon. Rather, it contains an acid–pyridine discrete N^{+}–H···O^{-} ionic synthon along with N–H···O and O–H···O hydrogen bonds between the remaining carboxylic acid groups of TACA and the amide group of the NA molecule. Non-planar TACA results in a helical hydrogen bonded network connecting the adjacent water and NA molecules (Fig. 2b). The water molecule actively takes part in connecting the helical TACA molecules using O–H···O hydrogen bonds (Fig. 2c). The conformation of one of the carboxylic acids of TACA is unusual; it exists in the *trans* form connecting the amide–carbonyl group of the NA molecule *via* an O–H···O hydrogen bond.

Crystallizing LAG samples of a 1 : 2 stoichiometric mixture of TACA–NA from tetrahydrofuran (THF) results in a needle shaped single crystal of the $(TACA)_2\cdot(NA)_4\cdot(H_2O)$ cocrystal with two molecules of TACA, four molecules of NA and one molecule of

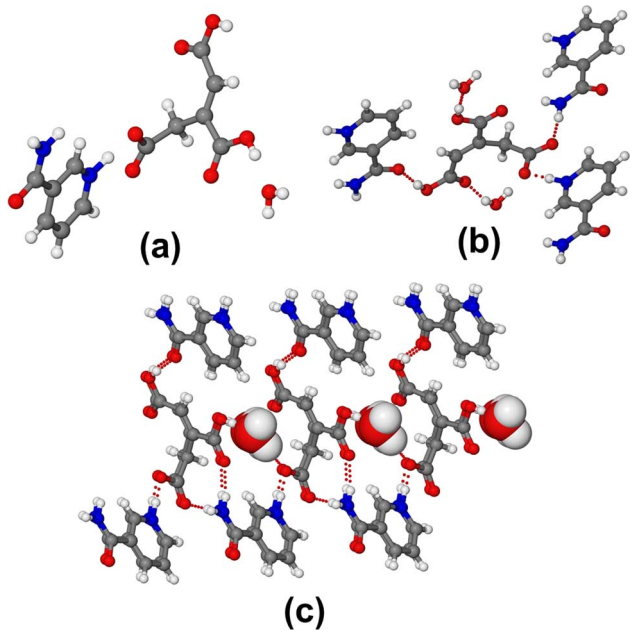

Fig. 2 (a) Molecules present in the asymmetric unit. (b) TACA molecule connected to adjacent NA and water using O–H···O and N–H···O/N^{+}–H···O^{-} hydrogen bonds. (c) Helical chain of TACA connected using an O–H···O hydrogen bond with the water molecule along with flanking NA connected on both sides. Packing diagrams are prepared from SCXRD data collected at 100 K.

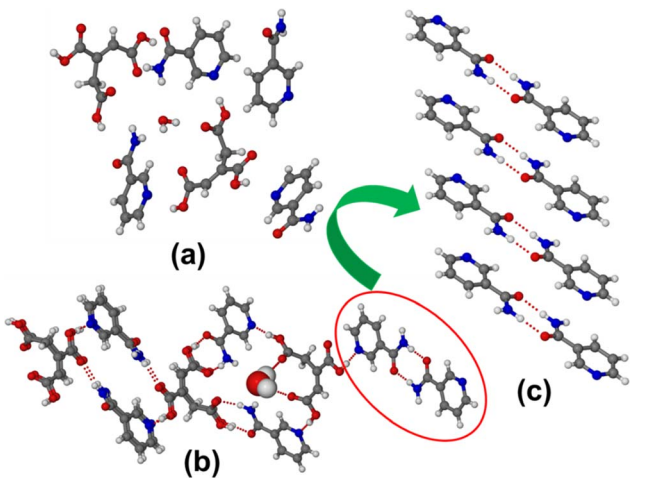

Fig. 3 (a) Molecules present in the asymmetric unit. (b) Various supramolecular synthons present in the $(TACA)_2\cdot(NA)_4\cdot(H_2O)$ form I cocrystal hydrate. (c) Amide-dimer synthon characteristic of form I.

water in the asymmetric unit (Fig. 3a). The crystal structure was solved in the triclinic $P\bar{1}$ space group. The $(TACA)_2\cdot(NA)_4\cdot(H_2O)$ molecular structure does not show any proton transfer from the acidic counterpart of TACA to NA and hence can be considered as a cocrystal hydrate. The conformations of all the carboxylic acid groups of TACA are *cis* (no *trans* form exists like in its 1 : 1 salt hydrate) and the two symmetry independent TACA molecules show different supramolecular synthons connected to adjacent NA molecules. The three carboxylic acid functionals of one TACA connect three neighboring NA molecules using acid–pyridine supramolecular synthons (O–H···N hydrogen bond). Two carboxylic acid groups of the second symmetry independent TACA unit form an acid–amide dimer synthon with their NA neighbors and the third carboxylic acid group connects two adjacent NAs using an acid–pyridine (O–H···N) and a discreet acid–amide N–H···O single point supramolecular synthon. The water molecule resides in the void created by the helical channel formed using a symmetry independent tetrameric TACA–NA unit *via* an O–H···O hydrogen bond, as shown in Fig. 3b. One of the symmetry independent NA molecules also contains a centrosymmetric amide dimer synthon that further connects neighboring TACA using an acid–pyridine O–H···N hydrogen bond synthon (Fig. 3b and c).

The comparison of the calculated powder patterns of 1 : 1 and 1 : 2 with the LAG material (ACN as liquid) confirms the 1 : 2 $(TACA)_2\cdot(NA)_4\cdot(H_2O)$ cocrystal hydrate (designated as form I hereafter) to be phase pure, whereas the 1 : 1 $(TACA)\cdot(NA)\cdot(H_2O)$ salt hydrate also contains traces of form I (see ESI Fig. S1†). Exploring neat grinding (NG) and LAG with various liquids, it was observed that the presence of water, isopropanol, THF, toluene and methanol results in the formation of a phase pure 1 : 1 molecular salt hydrate; on the other hand, LAG with hexane, ACN and EtOH always results in the concomitant formation of a 1 : 1 salt along with a 1 : 2 cocrystal (2θ peak at 13.3° characteristic of form I), confirmed using PXRD analysis (Fig. 4).

The influence of various added liquids during grinding shows the appearance of new PXRD patterns for 1 : 2 TACA–NA with ethanol, water and isopropanol (see ESI Fig. S2†). In order to characterize the material, solution crystallization was carried out for the ground powder in a mixture solvent of THF and methanol. Lath shaped single crystals obtained during slow evaporation confirm the material to be a polymorphic form of the $(TACA)_2\cdot(NA)_4\cdot(H_2O)$ cocrystal hydrate (hereafter designated as form II). PXRD analysis shows that LAG with hexane and ACN results in form I; LAG with water, ethanol and isopropanol yields form II, whereas LAG with all other liquids considered for the study results in the formation of concomitant polymorphic mixtures, as shown in ESI Fig. S2.†

Structural analysis showed that form II also contains two molecules of TACA, four molecules of NA and one water molecule in the asymmetric unit similar to form I and solved in the triclinic $P\bar{1}$ space group (Fig. 5a). Surprisingly, the two polymorphs have nearly identical crystal packing and hydrogen bond interactions. The form II structure also contains a symmetry independent TACA molecule connecting three neighboring NA molecules using an acid–pyridine O–H···N hydrogen bond synthon. The second TACA unit contains two acid–amide synthons connecting two NA molecules and one acid–pyridine synthon, as shown in Fig. 5b. The only difference

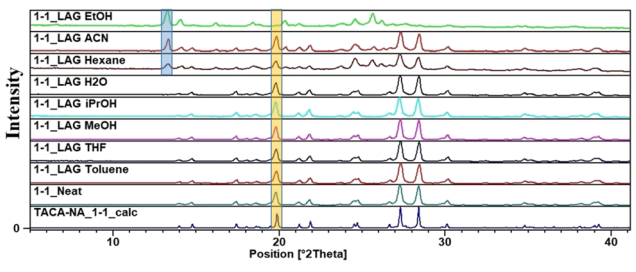

Fig. 4 PXRD pattern of the $(TACA)\cdot(NA)\cdot(H_2O)$ salt hydrate ground in the presence of various added liquids. Formation of a 1 : 2 cocrystal as an impurity in powder samples of a 1 : 1 mixture prepared using LAG with EtOH, ACN and hexane is confirmed based on the 2θ peak at 13.3° characteristic of form I shown using the blue line.

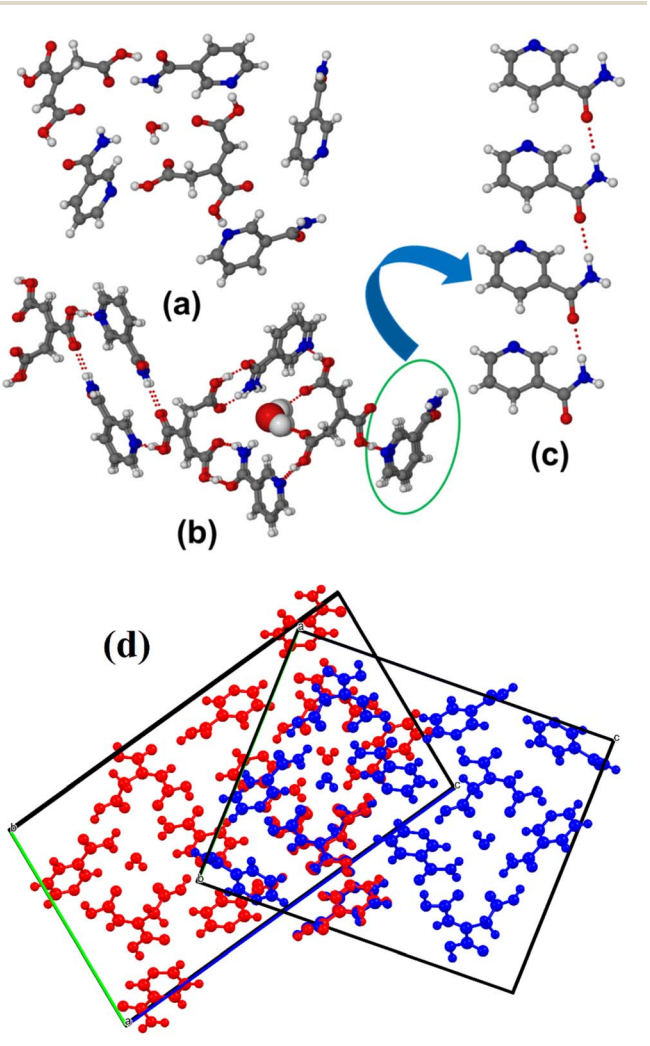

Fig. 5 (a) Molecules present in the asymmetric unit. (b) Various supramolecular synthons present in the $(TACA)_2\cdot(NA)_4\cdot(H_2O)$ form II cocrystal hydrate. (c) Amide catemer synthon characteristic of form II. (d) Crystal packing overlay of form I (red) and form II (blue) prepared using Mercury version 2024.1.0.

between the two structures is that in form II one of the NA molecules forms an amide catemer connecting adjacent NA molecules (Fig. 5c), whereas in form I, it instead forms a centrosymmetric amide dimer (Fig. 3c). The crystal packing similarity of form I and form II calculated using the licensed version of Mercury software showed a similarity of 5 out of 15 clusters with a PXRD similarity value of 0.297 and a rotation matrix value of 0.968. The crystal packing overlay of the two polymorphs is shown in Fig. 5d. FT-IR analysis also showed a clear difference between the stretching frequencies of the 1 : 1 (TACA)·(NA)·(H_2O) salt hydrate and 1 : 2 polymorphic (TACA)$_2$·(NA)$_4$·(H_2O) cocrystal hydrate (see ESI Fig. S3†). Although the number of structures with high Z' (the number of symmetry independent molecules in the asymmetric unit for a single component system) and Z'' (the number of symmetry independent molecules in the asymmetric unit for a multi-component system) has increased in recent years,[53,54] polymorphic systems with high Z'' are uncommon and only a few are reported in the literature.[55–61] The analysis of the Cambridge Crystallographic Database[62] (CSD; Conquest 2022.3.0 v. July 2023) shows the existence of only five dimorphic co-crystal hydrates to date, with the highest Z'' value of nine (see Table S1 in the ESI†).[63–67] Among the reported structures, most of them have different crystal packing arrangements and hydrogen bond interactions. Blagden *et al.* reported[68] three polymorphic cocrystals (Z'' values of 3, 3, and 6) and a concomitant salt structure (Z'' value of 3) for a closely related molecule citric acid with isonicotinamide, whereas a 1 : 2 cocrystal for citric acid with nicotinamide was observed during cocrystallization reported by Lemmerer and Bernstein.[69] In our case, the only major difference between the two polymorphs is the presence of amide dimeric (form I) and catemeric (form II) synthons between the nicotinamide molecules. We have also carried out a CSD search on the relative abundance of amide dimeric *vs.* catemeric synthons present in the reported literature. It shows that structures with only amide catemeric synthons are ~36% compared to molecules with only dimeric synthons (~43%). Approximately 21% of crystal structures contain both of them in their packing arrangement. The crystallographic information details and hydrogen bond parameters of the TACA–NA–H_2O multi-component solids are included in ESI, Tables S2 and S3.†

We also explored the effect of η (the volume of the liquid in μL divided by the sample weight in mg) during grinding on polymorphic phase transformation. PXRD analysis showed that LAG with ACN results in the formation of form I having an η value in the range 0.179–1.196 (15–100 μL), whereas an increase in the η value beyond 1.196 results in the formation of concomitant polymorphic mixtures (forms I and II), confirmed using PXRD analysis (see ESI Fig. S4†).

Turnover experiment

Next, we have checked whether form I and form II of the (TACA)$_2$·(NA)$_4$·(H_2O) cocrystal hydrate are interconvertible or not. At first, the LAG of (TACA)$_2$·(NA)$_4$·(H_2O) in the presence of hexane is performed, followed by recording the PXRD pattern of

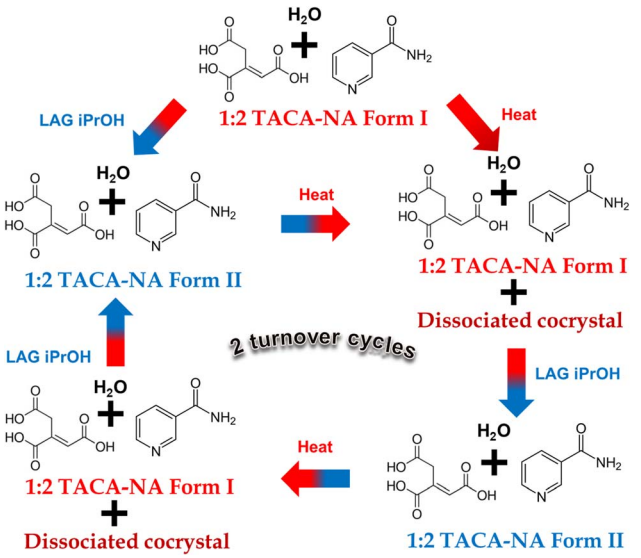

Scheme 2 Representation of the interconvertible nature of form I and form II of (TACA)$_2$·(NA)$_4$·(H_2O) along with the dissociated cocrystal upon heating.

the resultant mixture. The material was confirmed to be phase pure form I based on PXRD analysis (see ESI Fig. S5†). The same powder sample was then ground using isopropanol, showing a polymorphic phase transformation from form I to form II (Scheme 2; also see ESI Fig. S5†). The transformed form II powder was again subjected to grinding in the presence of hexane and characterized using PXRD. PXRD analysis showed that the material does not revert back to form I. However, heating the material at 80 °C for ~80 minutes leads to partial conversion to form I along with a few additional peaks corresponding to possible cocrystal dissociation (see the Stability of the stoichiometric/polymorphic multi-component solids section), as seen from characterization by PXRD (see ESI Fig. S4†). This polymorphic turnover experiment can be carried out in both clockwise and anticlockwise directions (based on the arrow direction as shown in Scheme 2) through two cycles and in duplicate to prove that these polymorphic transformations can be repeated as many times as desired and are reproducible with partial dissociation of the form I cocrystal (see ESI Fig. S6–S8†).

We have also checked whether the (TACA)$^-$·(NA)$^+$·(H_2O) molecular salt hydrate can be inter-convertible to the (TACA)$_2$·(NA)$_4$·(H_2O) cocrystal hydrate and *vice versa* or not. At first, a LAG sample of the (TACA)$^-$·(NA)$^+$·(H_2O) salt hydrate in the presence of water is prepared and the PXRD pattern is recorded to confirm its phase purity. Then to the resultant 1 : 1 mixture, 1 mol equivalent of NA was added and the powder sample was ground in the presence of different added liquids and their PXRD patterns were recorded. PXRD analysis confirms the resultant powder material to be (TACA)$_2$·(NA)$_4$·(H_2O) form II irrespective of the added liquid during grinding. When 1 mol equivalent of TACA was added to form II and LAG was performed in the presence of water as added liquid, PXRD analysis

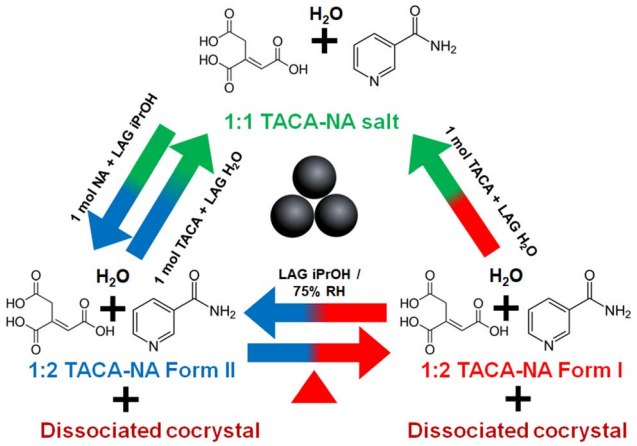

Scheme 3 Overall turnover experiment that shows the interconvertible nature of the 1 : 1 molecular salt hydrate and the two polymorphic 1 : 2 cocrystal hydrates along with cocrystal dissociation under various LAG conditions.

confirmed the transformation of form II to a 1 : 1 molecular salt hydrate, *i.e.*, the interconversion of a 1 : 1 molecular salt hydrate and 1 : 2 cocrystal hydrate is possible by means of grinding. Moreover, the form II material obtained from the addition of 1 mol equivalent of NA to the 1 : 1 salt hydrate material was placed in an oven at 80 °C for ~80 minutes, and form II further converted partially to form I along with a few additional peaks corresponding to possible dissociation of the 1 : 2 $(TACA)_2 \cdot (NA)_4 \cdot (H_2O)$ cocrystal. The transformed material (form I + dissociated cocrystal) can be further converted to a 1 : 1 molecular salt hydrate upon addition of 1 mol equivalent of TACA and subjecting to LAG in the presence of water (see ESI Fig. S9†). The turnover experiment of interconversion of a 1 : 1 molecular salt hydrate and 1 : 2 cocrystal hydrate can be repeated as many times as desired and is reproducible too.

Relative humidity (RH) study

We have also investigated the relative stability of the dimorphic $(TACA)_2 \cdot (NA)_4 \cdot (H_2O)$ 1 : 2 cocrystal hydrates under 75% RH.

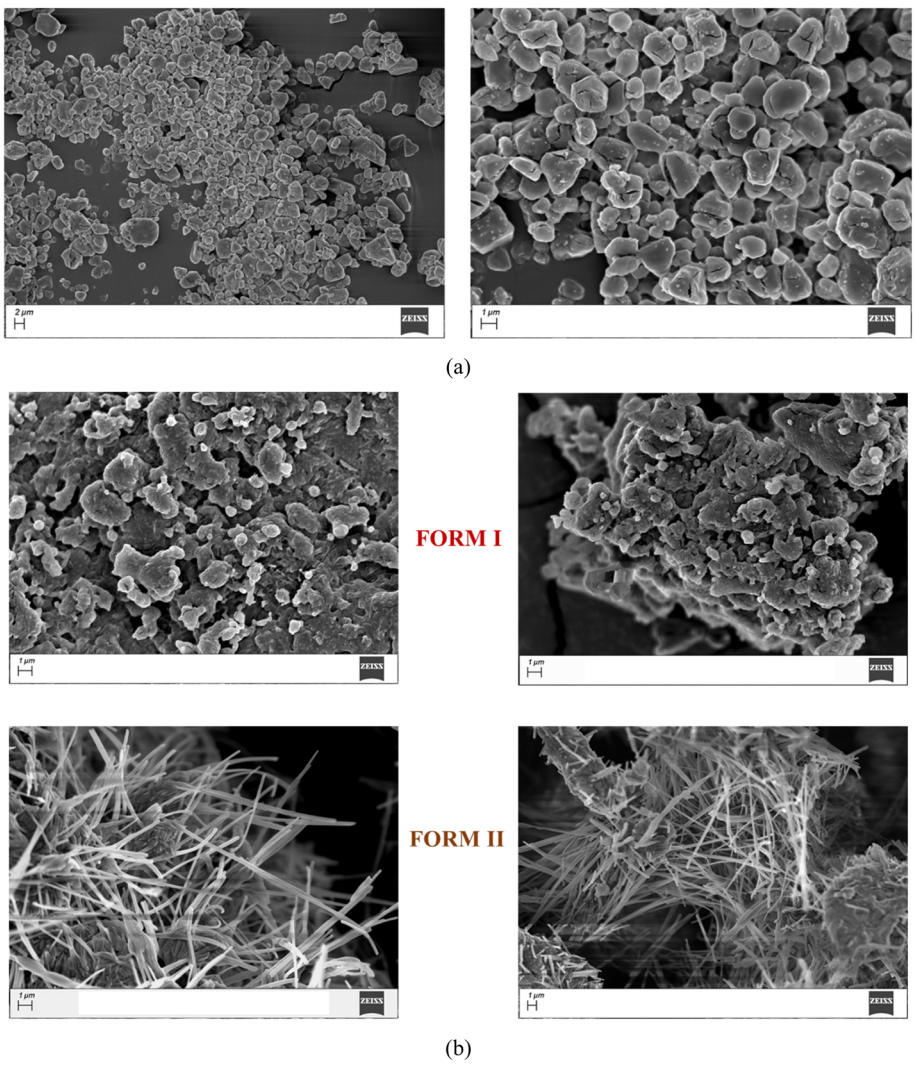

Fig. 6 SEM images of TACA–NA–H_2O: (a) 1 : 1 hydrated molecular salt and (b) 1 : 2 hydrated cocrystal form I and form II.

The powder samples of the respective 1 : 2 cocrystals were placed in bell jars containing saturated NaCl aqueous solution that maintains a relative humidity of 75% and their PXRD patterns were recorded after a regular interval of time. PXRD analysis showed the form II cocrystal to be stable, whereas form I, after a period of 1 week under 75% RH, was found to transform to form II along with the formation of a small amount of 1 : 1 molecular salt and pure TACA (see ESI, Fig. S10†). Finally, after a period of 3 months, ~70% of form I transformed to form II, along with 1 : 1 molecular salt and starting material, TACA, based on Rietveld refinement (see ESI Fig. S11†).

The overall turnover experiment of 1 : 1 molecular salt and 1 : 2 polymorphic cocrystal hydrates is illustrated in Scheme 3.

During the turnover experiment, we also observed that there is a significant morphological change of the particles of the respective 1 : 1 salt and polymorphic 1 : 2 cocrystal hydrates. The 1 : 1 salt hydrate shows the formation of irregular shaped particles with a size range of 2–3 μm. On the other hand, the 1 :

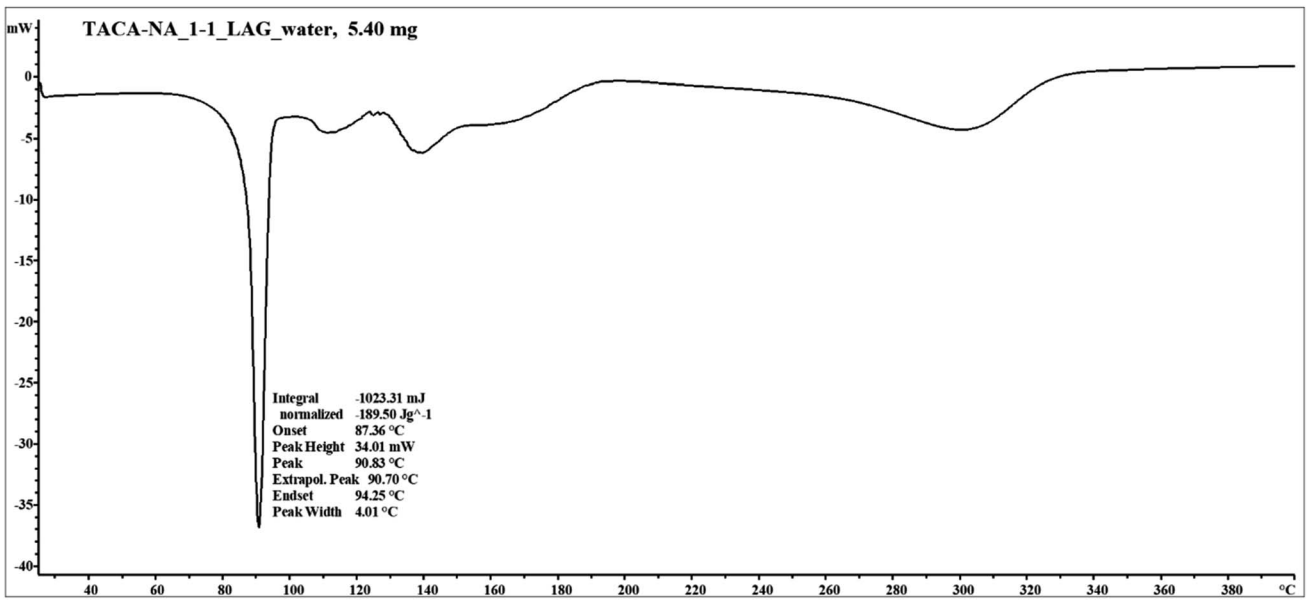

(a)

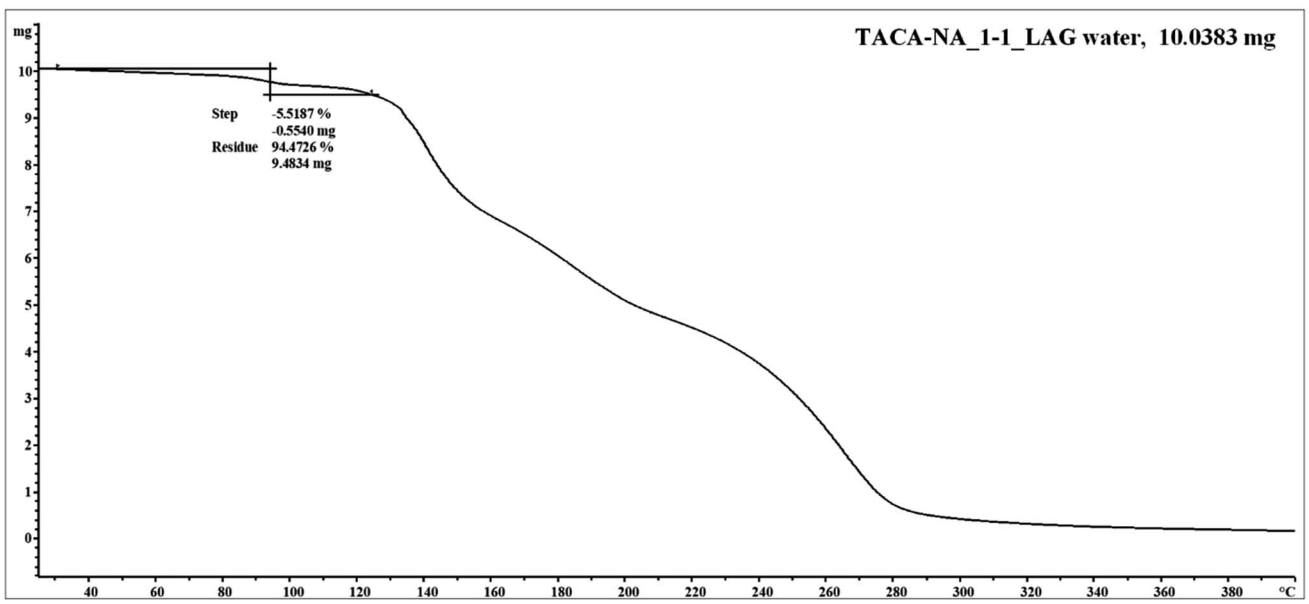

(b)

Fig. 7 (a) DSC and (b) TG thermograms of the 1 : 1 TACA–NA–H_2O hydrated molecular salt.

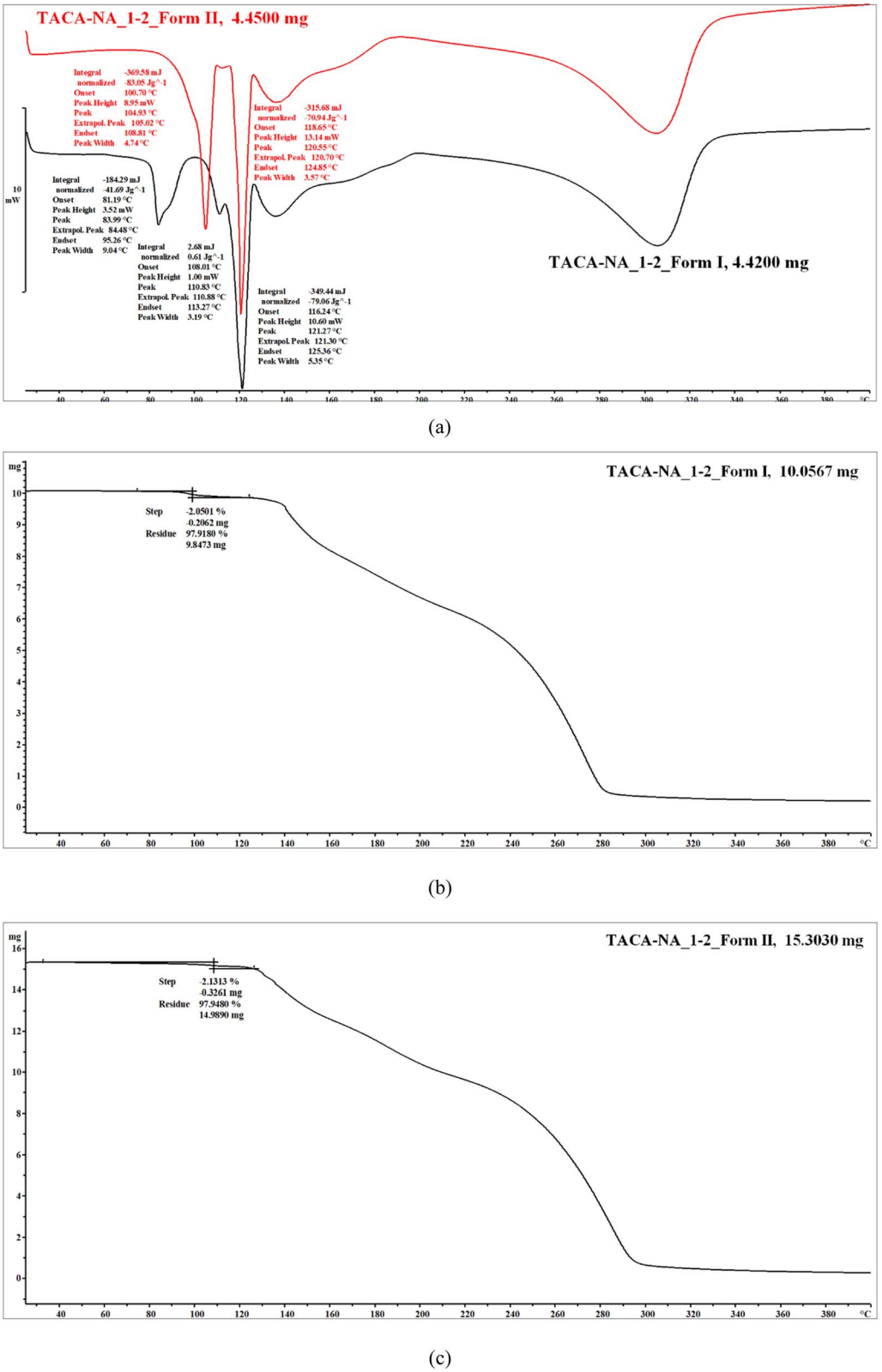

Fig. 8 (a) DSC and (b and c) TG thermograms of 1 : 2 TACA–NA–H_2O hydrated cocrystal form I and form II, respectively.

2 form I cocrystal hydrate shows the formation of aggregates with significantly larger particles during fresh preparation as well as interconversion. The 1 : 2 form II cocrystal hydrate shows the formation of well-defined long acicular particles during fresh preparation using LAG as well as interconversion from form I and/or the 1 : 1 molecular salt hydrate as evident from their FE-SEM images (Fig. 6 and ESI Fig. S12†).

Stability of the stoichiometric/polymorphic multi-component solids

Thermal measurements showed that the 1 : 1 TACA–NA hydrated molecular salt undergoes a loss of solvent water along with melting of the molecular salt, followed by the dissociation of the material. The DSC thermogram shows melting (onset) coupled with solvent water loss at 87 °C (Fig. 7). Thermogravimetric analysis (TGA) showed a weight loss of 5.5% corresponding to the loss of 1 mol equivalent of water, which matches well with the theoretical value.

The DSC thermogram of the 1 : 2 TACA–NA–H_2O form I cocrystal shows the loss of solvent water at 78 °C (onset) (Fig. 8a). If the cocrystal is exposed to 80 °C for a longer period, it shows two endothermic peaks. The first endothermic event at 107 °C may be a possible polymorphic phase transformation of the 1 : 2 guest-free form, followed by melting of the guest-free form at 116.19 °C. The weight loss of 2.1% observed in the TG curve (Fig. 8b) corresponds to 1 mol equivalent of water, which nicely coincides with the X-ray crystal structure (theoretical value: 2.1%). The form II cocrystal shows the loss of solvent water at 100.71 °C. The broader endothermic peak may be due

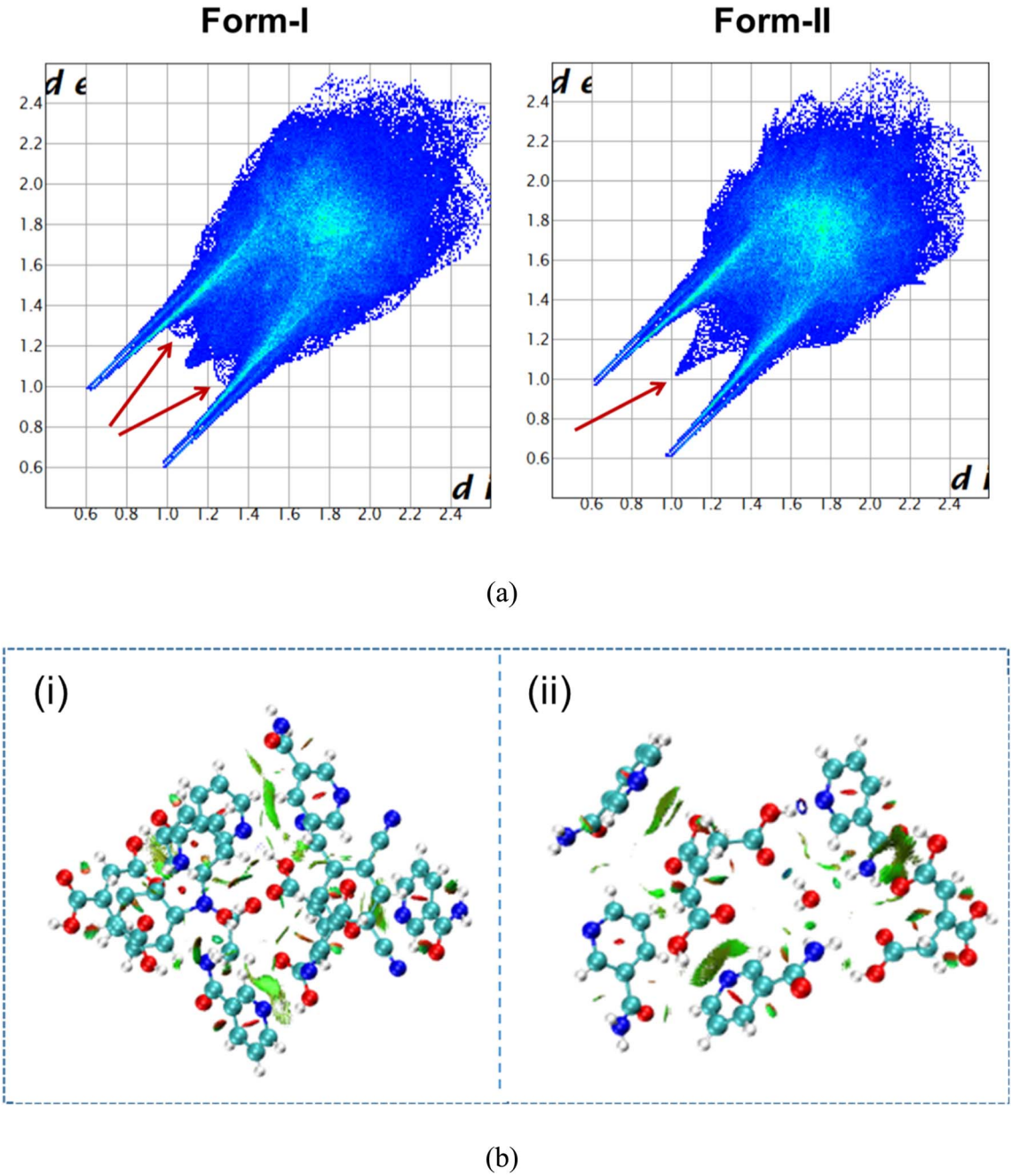

Fig. 9 (a) 2D-fingerprint plots of form I and form II clearly displaying the difference in intermolecular interactions present in the crystal structure shown using the red arrow; (b) non-covalent interaction plots of (i) form I and (ii) form II visualized at an isosurface value of 0.5.

Table 1 Lattice energy of polymorphic forms I and II calculated using Gaussian 16

Form	a (Å)	b (Å)	c (Å)	α (°)	β (°)	γ (°)	E_{pack} (kcal mol^{-1})	E_{SP} (kcal mol^{-1})	$E_{lattice}$ (kcal mol^{-1})
I	5.0306	14.9770	26.8120	84.727	87.615	87.464	−240.328697	−62.94923915	−303.28
II	5.0668	17.9930	22.1390	92.134	93.962	94.232	−240.876561	−58.409546	−299.29

to the overlap of the observed phase transformation event from form II to form I, further confirmed using PXRD analysis, followed by the loss of solvent water. It shows a single melting endotherm with the melting onset at 118 °C (Fig. 8a), which coincides with the second melting endotherm observed for the anhydrous 1 : 2 cocrystal. The weight loss of 2.08% observed in the TG curve (Fig. 8c) corresponds to 1 mol equivalent of water, which coincides with the theoretical value of 2.1% based on X-ray crystal structure analysis. In order to confirm the cocrystal dissociation, the form I material was also further heated at 90 °C for a period of ∼15 min and the PXRD pattern of the powder sample was recorded. The powder pattern exactly matches with the PXRD pattern of the heated form II material used for the turnover experiment (see ESI Fig. S13†). Moreover, the addition of a trace amount of TACA to the form I material during grinding shows exactly the same PXRD pattern obtained after heating form I as well as form II, which further supports our assumption of possible cocrystal dissociation.

Theoretical studies

Differences in the aqueous pK_a values (ΔpK_a) have been calculated to understand the salt formation in the 1 : 1 case and polymorphic cocrystals in the 1 : 2 case. Chemists and crystal engineers typically use the pK_a rule to cautiously predict the formation of molecular salts and cocrystals. Empirical data have revealed that for multi-component crystals comprising acid and basic constituents, ΔpK_a > 4 nearly invariably leads to salts, ΔpK_a < −1 almost always leads to cocrystals, and ΔpK_a between −1 and 4 can lead to either.[70–72]

We have used density functional theory (wb97xd/6-311++g(d,p)) to estimate the pK_a values. The combination of the wb97xd/6-311++g(d,p) method is used to optimize the molecules in the gaseous phase, while the SMD universal solvation model is used to optimize the solvated counterparts as implemented in the Gaussian 16 program package (see the ESI† for more details and optimized coordinates of individual conformers). This level of theory has been previously benchmarked as the best DFT functional for reliable pK_a calculations.[73,74] We have observed that ΔpK_a for the 1 : 1 case is 3.4 and 0.1 was obtained in the case of the 1 : 2 cocrystal system that resides in the grey region. Therefore, the formation of a molecular salt in the 1 : 1 case and cocrystal in 1 : 2 stoichiometric ratios of TACA and NA during manual grinding should be best explained using experimental SCXRD analysis.

In a quest to show the relative stability of form I and form II, lattice energy calculations are performed at the B3LYP-GD3/Def2TZVP level of theory. The gas phase DFT calculated lattice energy values are found to be very close (Table 1). Non-covalent interactions play a vital role in the crystal packing of organic crystals and, thereby, the stability of organic electronic materials. Hirshfeld surface analysis provides a better comparison of the intermolecular interactions present within a crystal structure. The 2D fingerprint plots of the two polymorphic systems show nearly identical non-covalent interactions. The two spikes corresponding to N···H and O···H contributions are identical in nature; the major difference is due to the van der Waals interactions corresponding to the H···H contribution that is shown using the arrow in red (Fig. 9a). Along with the quantitative analysis based on Hirshfeld surface analysis (see ESI Fig. S14†), non-covalent interactions in form I and form II are qualitatively visualized in Fig. 9b.

Conclusion

In conclusion, we have reported a one-pot reversible polymorph and variable stoichiometric multi-component solid of TACA and NA by manual grinding. A 1 : 1 stoichiometric ratio forms a molecular salt hydrate, whereas a 1 : 2 stoichiometric ratio of TACA and NA yields a rare dimorphic system of cocrystal hydrates with seven independent molecules in the asymmetric unit. All the multi-component solids are interconvertible and characterized using various solid-state techniques. All the multi-component solids show distinct morphologies based on their SEM micrographs. The turnover experiment showed that the form I cocrystal was prone to dissociation upon heating and in the presence of excess starting material (TACA) as an impurity during grinding. Density functional theory ΔpK_a calculations show the values in the grey region. Therefore, SCXRD plays an important role in establishing the formation of a molecular salt in the case of a 1 : 1 TACA–NA mixture and cocrystal formation during milling of a TACA and NA mixture in a 1 : 2 stoichiometric ratio. Also, lattice energy calculations showed that the two polymorphic systems are within a close energy window with form I being thermodynamically stable in the gas phase. However, it is difficult to summarize their relative stability as during LAG experiments, most of the liquids resulted in the formation of concomitant mixtures of forms I and II; the crystal densities of the two polymorphs are also nearly equal. Although thermal measurements showed the transformation of form II to form I at high temperatures, high humidity resulted in their interconversion. We hope that such in-depth analysis based on mechanochemistry will improve our understanding of the structural landscape of multi-component solids prior to pharmaceutical cocrystal/salt design and avoid unwanted polymorphs or multi-component solids as impurities during batch formulation.

Data availability

All the data with respect to the manuscript are available with the authors and can be shared if required with the journal authority. The crystallographic data are already uploaded to the CSD and can be downloaded as the ESI† from the website.

Conflicts of interest

The authors declare no competing financial interest.

Acknowledgements

R. C. D. and R. T. thank the Science and Engineering Research Board for funding under the Teachers Associateship for Research Excellence (TARE) grant (Project No. TAR/2021/000251). M. A. thanks the National Science Center of Poland (NCN) for the financial support *via* OPUS grant 2020/37/B/ST5/02638. We gratefully acknowledge the Sophisticated Analytical Instrumentation Facility (SAIF), GU, for the provision of the single crystal X-ray diffractometer and the Department of Chemistry, GU, for the Rigaku powder X-ray diffractometer, basic instrumentation facility, and infrastructure. We thank Dr Tejender S. Thakur for collecting single crystal data of the TACA–NA molecular salt at 100 K.

References

1 F. Gomollón-Bel, Ten Chemical Innovations That Will Change Our World: IUPAC Identifies Emerging Technologies in Chemistry with Potential to Make Our Planet More Sustainable, *Chem. Int.*, 2019, **41**, 12–17.
2 A. M. Belenguer, T. Friščić, G. M. Day and J. K. M. Sanders, Solid-state dynamic combinatorial chemistry: reversibility and thermodynamic product selection in covalent mechanosynthesis, *Chem. Sci.*, 2011, **2**, 696–700.
3 A. M. Belenguer, G. I. Lampronti, A. A. L. Michalchuk, F. Emmerling and J. K. M. Sanders, Quantitative reversible one pot interconversion of three crystalline polymorphs by ball mill grinding, *CrystEngComm*, 2022, **24**, 4256–4261.
4 I. A. Tumanov, A. F. Achkasov, E. V. Boldyreva and V. V. Boldyrev, Following the products of mechanochemical synthesis step by step, *CrystEngComm*, 2011, **13**, 2213–2216.
5 E. Losev, S. Arkhipov, D. Kolybalov, A. Mineev, A. Ogienko, E. Boldyreva and V. Boldyrev, Substituting steel for a polymer in a jar for ball milling does matter, *CrystEngComm*, 2022, **24**, 1700–1703.
6 L. S. Germann, M. Arhangelskis, M. Etter, R. E. Dinnebier and T. Friščić, Challenging the Ostwald rule of stages in mechanochemical cocrystallisation, *Chem. Sci.*, 2020, **11**, 10092–10100.
7 J.-L. Do and T. Friščić, Mechanochemistry: A Force of Synthesis, *ACS Cent. Sci.*, 2017, **3**, 13–19.
8 A. A. L. Michalchuk, I. A. Tumanov and E. V. Boldyreva, Complexities of mechanochemistry: elucidation of processes occurring in mechanical activators *via* implementation of a simple organic system, *CrystEngComm*, 2013, **15**, 6403–6412.
9 N. Bouvart, R.-M. Palix, S. G. Arkhipov, I. A. Tumanov, A. A. L. Michalchuk and E. V. Boldyreva, Polymorphism of chlorpropamide on liquid-assisted mechanical treatment: choice of liquid and type of mechanical treatment matter, *CrystEngComm*, 2018, **20**, 1797–1803.
10 V. V. Boldyrev, S. V. Pavlov and E. L. Goldberg, Interrelation between fine grinding and mechanical activation, *Int. J. Miner. Process.*, 1996, **44–45**, 181–185.
11 F. Fischer, S. Greiser, D. Pfeifer, C. Jäger, K. Rademann and F. Emmerling, Mechanochemically Induced Conversion of Crystalline Benzamide Polymorphs by Seeding, *Angew. Chem., Int. Ed.*, 2016, **55**, 14281–14285.
12 D.-K. Bučar, G. M. Day, I. Halasz, G. G. Z. Zhang, J. R. G. Sander, D. G. Reid, L. R. MacGillivray, M. J. Duer and W. Jones, The curious case of (caffeine)·(benzoic acid): how heteronuclear seeding allowed the formation of an elusive cocrystal, *Chem. Sci.*, 2013, **4**, 4417–4425.
13 M. Arhangelskis, D.-K. Bučar, S. Bordignon, M. R. Chierotti, S. A. Stratford, D. Voinovich, W. Jones and D. Hasa, Mechanochemical reactivity inhibited, prohibited and reversed by liquid additives: examples from crystal-form screens, *Chem. Sci.*, 2021, **12**, 3264–3269.
14 D. Hasa, G. Schneider Rauber, D. Voinovich and W. Jones, Cocrystal Formation through mechanochemistry: from Neat and Liquid-Assisted Grinding to Polymer-Assisted Grinding, *Angew. Chem., Int. Ed.*, 2015, **54**, 7371–7375.
15 D. Cinčić, I. Brekalo and B. Kaitner, Solvent-Free Polymorphism Control in a Covalent Mechanochemical Reaction, *Cryst. Growth Des.*, 2012, **12**, 44–48.
16 D. Hasa, E. Miniussi and W. Jones, Mechanochemical Synthesis of Multicomponent Crystals: One Liquid for One Polymorph? A Myth to Dispel, *Cryst. Growth Des.*, 2016, **16**, 4582–4588.
17 H. Kulla, F. Fischer, S. Benemann, K. Rademann and F. Emmerling, The effect of the ball to reactant ratio on mechanochemical reaction times studied by *in situ* PXRD, *CrystEngComm*, 2017, **19**, 3902–3907.
18 F. Fischer, N. Fendel, S. Greiser, K. Rademann and F. Emmerling, Impact Is Important—Systematic Investigation of the Influence of Milling Balls in Mechanochemical Reactions, *Org. Process Res. Dev.*, 2017, **21**, 655–659.
19 A. A. L. Michalchuk, I. A. Tumanov and E. V. Boldyreva, Ball size or ball mass – what matters in organic mechanochemical synthesis?, *CrystEngComm*, 2019, **21**, 2174–2179.
20 K. Linberg, B. Röder, D. Al-Sabbagh, F. Emmerling and A. A. L. Michalchuk, Thermal control of mechanochemical polymorphism in organic cocrystals, *Faraday Discuss.*, 2023, **241**, 178–193.
21 A. A. L. Michalchuk, K. S. Hope, S. R. Kennedy, M. V. Blanco, E. V. Boldyreva and C. R. Pulham, Ball-free mechanochemistry: *in situ* real-time monitoring of pharmaceutical co-crystal formation by resonant acoustic mixing, *Chem. Commun.*, 2018, **54**, 4033–4036.

22 Y. Teoh, G. Ayoub, I. Huskić, H. M. Titi, C. W. Nickels, B. Herrmann and T. Friščić, SpeedMixing: Rapid Tribochemical Synthesis and Discovery of Pharmaceutical Cocrystals without Milling or Grinding Media, *Angew. Chem., Int. Ed.*, 2022, e202206293.
23 P. Sharma, C. Vetter, E. Ponnusamy and E. Colacino, Assessing the Greenness of Mechanochemical Processes with the DOZN 2.0 Tool, *ACS Sustainable Chem. Eng.*, 2022, **10**, 5110–5116.
24 F. Cuccu, L. De Luca, F. Delogu, E. Colacino, N. Solin, R. Mocci and A. Porcheddu, Mechanochemistry: New Tools to Navigate the Uncharted Territory of "Impossible" Reactions, *ChemSusChem*, 2022, **15**, e202200362.
25 E. Colacino, A. Porcheddu, I. Halasz, C. Charnay, F. Delogu, R. Guerra and J. Fullenwarth, Mechanochemistry for "no solvent, no base" preparation of hydantoin-based active pharmaceutical ingredients: nitrofurantoin and dantrolene, *Green Chem.*, 2018, **20**, 2973–2977.
26 P. J. Beldon, L. Fábián, R. S. Stein, A. Thirumurugan, A. K. Cheetham and T. Friščić, Rapid Room-Temperature Synthesis of Zeolitic Imidazolate Frameworks by Using Mechanochemistry, *Angew. Chem., Int. Ed.*, 2010, **49**, 9640–9643.
27 K. Užarević, T. C. Wang, S.-Y. Moon, A. M. Fidelli, J. T. Hupp, O. K. Farha and T. Friščić, Mechanochemical and solvent-free assembly of zirconium-based metal–organic frameworks, *Chem. Commun.*, 2016, **52**, 2133–2136.
28 T. Friščić, New opportunities for materials synthesis using mechanochemistry, *J. Mater. Chem.*, 2010, **20**, 7599–7605.
29 B. P. Biswal, S. Chandra, S. Kandambeth, B. Lukose, T. Heine and R. Banerjee, Mechanochemical Synthesis of Chemically Stable Isoreticular Covalent Organic Frameworks, *J. Am. Chem. Soc.*, 2013, **135**, 5328–5331.
30 S. T. Emmerling, L. S. Germann, P. A. Julien, I. Moudrakovski, M. Etter, T. Friščić, R. E. Dinnebier and B. V. Lotsch, *In situ* monitoring of mechanochemical covalent organic framework formation reveals templating effect of liquid additive, *Chem*, 2021, **7**, 1639–1652.
31 P. Zhang and S. Dai, Mechanochemical synthesis of porous organic materials, *J. Mater. Chem. A*, 2017, **5**, 16118–16127.
32 S. Karki, T. Friščić, W. Jones and W. D. S. Motherwell, Screening for Pharmaceutical Cocrystal Hydrates *via* Neat and Liquid-Assisted Grinding, *Mol. Pharmaceutics*, 2007, **4**, 347–354.
33 S. L. James, C. J. Adams, C. Bolm, D. Braga, P. Collier, T. Friščić, F. Grepioni, K. D. M. Harris, G. Hyett, W. Jones, A. Krebs, J. Mack, L. Maini, A. G. Orpen, I. P. Parkin, W. C. Shearouse, J. W. Steed and D. C. Waddell, Mechanochemistry: opportunities for new and cleaner synthesis, *Chem. Soc. Rev.*, 2012, **41**, 413–447.
34 N. Tumanova, N. Tumanov, K. Robeyns, F. Fischer, L. Fusaro, F. Morelle, V. Ban, G. Hautier, Y. Filinchuk, J. Wouters, T. Leyssens and F. Emmerling, Opening Pandora's Box: Chirality, Polymorphism, and Stoichiometric Diversity in Flurbiprofen/Proline Cocrystals, *Cryst. Growth Des.*, 2018, **18**, 954–961.
35 D. Hasa and W. Jones, Screening for new pharmaceutical solid forms using mechanochemistry: a practical guide, *Adv. Drug Delivery Rev.*, 2017, **117**, 147–161.
36 A. Delori, T. Friščić and W. Jones, The role of mechanochemistry and supramolecular design in the development of pharmaceutical materials, *CrystEngComm*, 2012, **14**, 2350–2362.
37 J.-R. Wang, C. Ye, B. Zhu, C. Zhou and X. Mei, Pharmaceutical cocrystals of the anti-tuberculosis drug pyrazinamide with dicarboxylic and tricarboxylic acids, *CrystEngComm*, 2015, **17**, 747–752.
38 N. Nagel, U. Endruschat and H. Bock, *cis*-Aconitic Acid at 150 K, *Acta Crystallogr., Sect. C: Cryst. Struct. Commun.*, 1996, **52**, 2912–2915.
39 Z. Yang, Y. Yang, M. Xia, W. Dai, B. Zhu and X. Mei, Improving the dissolution behaviors and bioavailability of abiraterone acetate *via* multicomponent crystal forms, *Int. J. Pharm.*, 2022, **614**, 121460.
40 I. J. Sugden, D. E. Braun, D. H. Bowskill, C. S. Adjiman and C. C. Pantelides, Efficient Screening of Coformers for Active Pharmaceutical Ingredient Cocrystallization, *Cryst. Growth Des.*, 2022, **22**, 4513–4527.
41 G. M. Sheldrick, *Program name*, University of Göttingen, Germany, 1996.
42 G. Sheldrick, Crystal structure refinement with SHELXL, *Acta Crystallogr., Sect. C: Struct. Chem.*, 2015, **71**, 3–8.
43 L. J. Barbour, X-Seed — A Software Tool for Supramolecular Crystallography, *J. Supramol. Chem.*, 2001, **1**, 189–191.
44 C. F. Macrae, P. R. Edgington, P. McCabe, E. Pidcock, G. P. Shields, R. Taylor, M. Towler and J. van de Streek, Mercury: visualization and analysis of crystal structures, *J. Appl. Crystallogr.*, 2006, **39**, 453–457.
45 A. Delori, P. T. A. Galek, E. Pidcock and W. Jones, Quantifying Homo- and Heteromolecular Hydrogen Bonds as a Guide for Adduct Formation, *Chem.–Eur. J.*, 2012, **18**, 6835–6846.
46 A. Delori, P. T. A. Galek, E. Pidcock, M. Patni and W. Jones, Knowledge-based hydrogen bond prediction and the synthesis of salts and cocrystals of the anti-malarial drug pyrimethamine with various drug and GRAS molecules, *CrystEngComm*, 2013, **15**, 2916–2928.
47 A. V. Trask, J. van de Streek, W. D. S. Motherwell and W. Jones, Achieving Polymorphic and Stoichiometric Diversity in Cocrystal Formation: Importance of Solid-State Grinding, Powder X-ray Structure Determination, and Seeding, *Cryst. Growth Des.*, 2005, **5**, 2233–2241.
48 S. Skovsgaard and A. D. Bond, Co-crystallisation of benzoic acid derivatives with N-containing bases in solution and by mechanical grinding: stoichiometric variants, polymorphism and twinning, *CrystEngComm*, 2009, **11**, 444–453.
49 S. Karki, T. Friščić and W. Jones, Control and interconversion of cocrystal stoichiometry in grinding: stepwise mechanism for the formation of a hydrogen-bonded cocrystal, *CrystEngComm*, 2009, **11**, 470–481.

50 H. Abourahma, D. D. Shah, J. Melendez, E. J. Johnson and K. T. Holman, A Tale of Two Stoichiometrically Diverse Cocrystals, *Cryst. Growth Des.*, 2015, **15**, 3101–3104.
51 S. Aitipamula, P. S. Chow and R. B. H. Tan, Polymorphism in cocrystals: a review and assessment of its significance, *CrystEngComm*, 2014, **16**, 3451–3465.
52 B. Saikia, D. Pathak and B. Sarma, Variable stoichiometry cocrystals: occurrence and significance, *CrystEngComm*, 2021, **23**, 4583–4606.
53 K. M. Steed and J. W. Steed, Packing Problems: High Z' Crystal Structures and Their Relationship to Cocrystals, Inclusion Compounds, and Polymorphism, *Chem. Rev.*, 2015, **115**, 2895–2933.
54 **https://zprime.co.uk/**.
55 H.-S. Shieh, L. G. Hoard and C. E. Nordman, Structures of triclinic and monoclinic cholesterol hemiethanolate, *Acta Crystallogr., Sect. B: Struct. Crystallogr. Cryst. Chem.*, 1982, **38**, 2411–2419.
56 A. S. Batsanov, J. C. Collings, R. M. Ward, A. E. Goeta, L. Porrès, A. Beeby, J. A. K. Howard, J. W. Steed and T. B. Marder, Crystal engineering with ethynylbenzenes Part 2. Structures of 4-trimethylsilylethynyl-*N*,*N*-dimethylaniline, and 4-ethynyl-*N*,*N*-dimethylaniline with $Z' = 12$ and a single-crystal to single-crystal phase transition at 122.5 ± 2 K, *CrystEngComm*, 2006, **8**, 622–628.
57 D. A. Parrish, J. R. Deschamps, R. D. Gilardi and R. J. Butcher, Polymorphs of Picryl Bromide, *Cryst. Growth Des.*, 2008, **8**, 57–62.
58 A. Lemmerer and M. A. Fernandes, Adventures in co-crystal land: high Z', stoichiometric variations, polymorphism and phase transitions in the co-crystals of four liquid and solid cyclic carboxylic acids with the supramolecular reagent isonicotinamide, *New J. Chem.*, 2012, **36**, 2242–2252.
59 Y. Yan, C. E. Hughes, B. M. Kariuki and K. D. M. Harris, A Rare Case of Polymorphism in a Three-Component Co-Crystal System, with Each Polymorph Having Ten Independent Molecules in the Asymmetric Unit, *Cryst. Growth Des.*, 2013, **13**, 27–30.
60 V. Palanisamy, P. Sanphui, G. Bolla, A. Narayan, C. C. Seaton and V. R. Vangala, Intriguing High Z'' Cocrystals of Emtricitabine, *Cryst. Growth Des.*, 2020, **20**, 4886–4891.
61 H. Liu, H. C. S. Chan, X. Yu, J. Li, J. Li and Z. Zhou, Two Polymorphic Cocrystals of Theophylline with Ferulic Acid, *Cryst. Growth Des.*, 2023, **23**, 4448–4459.
62 C. R. Groom and F. H. Allen, The Cambridge Structural Database in Retrospect and Prospect, *Angew. Chem., Int. Ed.*, 2014, **53**, 662–671.
63 M. K. Chantooni, D. Britton and I. M. Kolthoff, X-ray crystal structure of the 1:2:2 pentaethyleneglycol dimethyl ether(pentaglyme):dichloropicric acid:water complex. Infrared studies of the 1:2:2 complexes with tri-, tetra-, and pentaglyme, *J. Crystallogr. Spectrosc. Res.*, 1993, **23**, 497–503.
64 S. Aitipamula, A. B. H. Wong, P. S. Chow and R. B. H. Tan, Novel solid forms of the anti-tuberculosis drug, isoniazid: ternary and polymorphic cocrystals, *CrystEngComm*, 2013, **15**, 5877–5887.
65 M. V. Sosa-Rivadeneyra, P. Venkatesan, F. Flores-Manuel, S. Bernès, H. Höpfl, M. Cerón, S. Thamotharan and M. J. Percino, Quantitative analysis of intermolecular interactions in cocrystals and a pair of polymorphous cocrystal hydrates from 1,4-dihydroquinoxaline-2,3-dione and 1H-benzo[*d*]imidazol-2(3*H*)-one with 2,5-dihydroxy-1,4-benzoquinones: a combined X-ray structural and theoretical analysis, *CrystEngComm*, 2020, **22**, 6645–6660.
66 B. Zhou, Q. Zhao, L. Tang and D. Yan, Tunable room temperature phosphorescence and energy transfer in ratiometric co-crystals, *Chem. Commun.*, 2020, **56**, 7698–7701.
67 C. Fiore, A. Baraghini, O. Shemchuk, V. Sambri, M. Morotti, F. Grepioni and D. Braga, Inhibition of the Antibiotic Activity of Cephalosporines by Co-Crystallization with Thymol, *Cryst. Growth Des.*, 2022, **22**, 1467–1475.
68 P. Stainton, T. Grecu, J. McCabe, T. Munshi, E. Nauha, I. J. Scowen and N. Blagden, First Comparative Study of the Three Polymorphs of Bis(isonicotinamide) Citric Acid Cocrystals and the Concomitant Salt 4-Carbamoylpyridinium Citrate Isonicotinamide, *Cryst. Growth Des.*, 2018, **18**, 4150–4159.
69 A. Lemmerer and J. Bernstein, The co-crystal of two GRAS substances: (citric acid)·(nicotinamide). Formation of four hydrogen bonding heterosynthons in one co-crystal, *CrystEngComm*, 2010, **12**, 2029–2033.
70 A. J. Cruz-Cabeza, Acid–base crystalline complexes and the pK_a rule, *CrystEngComm*, 2012, **14**, 6362–6365.
71 T. Wang, J. S. Stevens, T. Vetter, G. F. S. Whitehead, I. J. Vitorica-Yrezabal, H. Hao and A. J. Cruz-Cabeza, Salts, Cocrystals, and Ionic Cocrystals of a "Simple" Tautomeric Compound, *Cryst. Growth Des.*, 2018, **18**, 6973–6983.
72 A. J. Cruz-Cabeza, M. Lusi, H. P. Wheatcroft and A. D. Bond, The role of solvation in proton transfer reactions: implications for predicting salt/co-crystal formation using the ΔpK_a rule, *Faraday Discuss.*, 2022, **235**, 446–466.
73 R. W. Pereira and R. O. Ramabhadran, pK-Yay: A Black-Box Method Using Density Functional Theory and Implicit Solvation Models to Compute Aqueous pKa Values of Weak and Strong Acids, *J. Phys. Chem. A*, 2020, **124**, 9061–9074.
74 J. R. Pliego Jr, Thermodynamic cycles and the calculation of pK_a, *Chem. Phys. Lett.*, 2003, **367**, 145–149.